

## Nickel-promoted Fabrication of Multicrystalline Carbon Nanotubes with Improved Electrochemical Capacitance

Zhong Zheng,<sup>\*1</sup> Dongguo Li,<sup>2</sup> Li He,<sup>1</sup> Jiaji Zhang,<sup>1</sup> and Xiaomin Ni<sup>2</sup>

<sup>1</sup>Department of Electronic Science and Technology, University of Science and Technology of China, Hefei, Anhui 230027, P. R. China

<sup>2</sup>Department of Chemistry, University of Science and Technology of China, Hefei, Anhui 230026, P. R. China

(Received May 1, 2007; CL-070470; E-mail: zozheng@ustc.edu.cn)

Novel carbon nanotubes (CNTs) with multicrystalline tube walls were fabricated by pyrolyzing acetone with single-crystalline nickel nanoflakes as promoter. Thus-prepared CNTs exhibited high specific capacitance and excellent cyclic stability without any activation treatments, which was ascribed to their special structures.

Electrochemical supercapacitors (ESC) has been of great interest for their practical applications as high power devices with merits of large capacitance, long cycling life, and charging and discharging with large electric current free of destroying.<sup>1,2</sup> Among the various materials suitable for the fabrication of electrodes of ESC, carbon nanotubes (CNTs) attracted special attention for their novel hollow-tube structure, nanometer dimension, high specific surface, and excellent electronic semi-conductivity and conductivity.<sup>3,4</sup> However, the pristine CNTs always displayed low capacitance because their active surface area for forming the electric double layer was smaller than the real surface area.<sup>5</sup> In order to improve the performance, activation treatments were usually performed, such as calcining CNTs with KOH in nitrogen or refluxing in HNO<sub>3</sub>, which can enlarge the micropores into well accessible mesopores, open the tips and break the long tubes into shorter ones, or modify the tube surface with some functional groups to influence their electronic structure.<sup>6</sup> Although these activation pretreatments can effectively improve the capacitance of CNTs; however, they usually involved special equipment and complicated procedures. In this paper, we reported a new kind of CNTs with multicrystalline tube walls, which exhibited high capacitance and excellent cyclic stability without any activation treatments. The crystalline CNTs were fabricated by catalytic decomposition of acetone with the promoter of single-crystalline nickel nanoflakes which we prepared before.<sup>7</sup> The key factors affecting the formation of the multicrystalline CNTs and their good electrochemical performances as electrochemical double-layered supercapacitors (EDLSCs) were investigated.

The single-crystalline nickel nanoflakes with hexagonal shapes were prepared by the procedures reported in our previous paper.<sup>7</sup> For the fabrication of carbon nanotubes, 20 mg of thus-prepared nickel powder was added into a 20-mL stainless autoclave containing 12 mL of acetone. Subsequently, the autoclave was sealed and heated at 600 °C for 12 h. The resulted black powders were collected and treated with dilute HNO<sub>3</sub> solution to remove the nickel nanoflakes. Then, the powder was rinsed and vacuum dried before use.

X-ray diffraction was carried out on a Philips X'Pert Super diffractometer with graphite monochromatized Cu K $\alpha$  radiation

( $\lambda = 1.54178 \text{ \AA}$ ). Structure and morphology of the products were examined by field emission scanning electron microscopy (FE-SEM, JEOL JSM-6300F), transmission electron microscopy (TEM, Hitachi 800) and high-resolution transmission electron microscopy (HRTEM, JEOL-2010). The electrochemical capacitance of the sample was tested using a symmetrical cell configuration in the galvanostatic charge-discharge model with the constant current of 5 mA.

Figure 1 showed the XRD pattern of the sample, in which four diffraction peaks could be indexed as (002), (100), (101), and (004) crystal plane diffractions of graphite carbon (JCPDS: 41-1487). No peaks of other impurities were detected, indicating that pure graphite carbon was fabricated under the current synthetic procedures.

Figure 2a showed a panoramic SEM image and the corresponding TEM image of the sample, revealing that randomly entangled CNTs with the length of several microns and the diameter of about 80–100 nm were obtained under the promotion by nickel nanoflakes with hexagonal shape. According to the SEM observations, the proportion of CNTs in the product was above 95%, implying the high catalytic efficiency of the single-crystalline nickel nanoflakes. TEM image of Figure 2b demonstrated the middle and tip parts of a typical CNT, indicating that the tube had open ends and multicrystalline walls with the gap size of about 5–10 nm. The wall thickness of the CNTs was about 20 nm and the inner diameter was about 50 nm. HRTEM image of Figure 2c revealed that the graphite layers were all perpendicular to the tube axis, which spontaneously coiled into tubes. Such a structural characteristic was much different from that of the common CNTs with the graphite layers oriented along the tube axis. For contrast, we studied the structure of the CNTs promoted by nickel nanoparticles instead of the nanoflakes keeping the other conditions same. Morphological images of Figures 2d and 2e indicated that these CNTs had

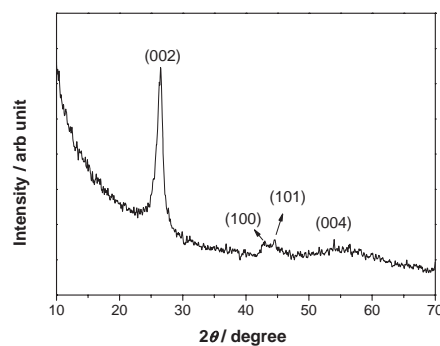
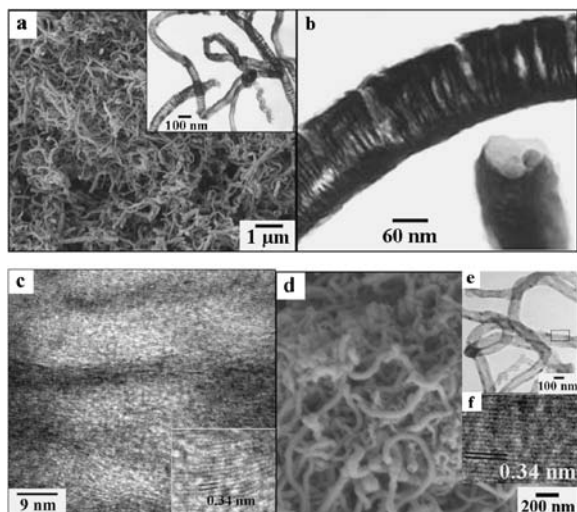


Figure 1. XRD pattern of the sample.



**Figure 2.** (a) FESEM image of the creviced CNTs, inset was the corresponding TEM image. (b) TEM image of the middle and end parts of a typical CNT. (c) HRTEM image of the tube wall, inset was a magnified image of the lattice fringes. (d) SEM image and TEM image (e) of the CNTs promoted by nickel nanoparticles. (f) HRTEM image of the part framed in Figure 2e.

continuous tube walls without any crevices. Figure 2f was a lattice-resolved HRTEM image of the part framed in Figure 2e, showing the graphite layers parallel to the axis of the CNT. Such multi-creviced CNTs were similar to the cup-stacked-type CNTs fabricated by a floating reactant method.<sup>8</sup>

The shape of the catalyst was an important factor affecting the morphology of the CNTs. Because the other experimental conditions are equal, formation of the novel creviced CNTs could be rationally ascribed to the special single-crystalline nickel nanoflakes. In the obtained CNTs before the acid treatment, we found that the nickel particles encapsulated in the tips still emerged as the single-crystalline hexagonal flake (seen the Supporting Information 1).<sup>14</sup> It was known that the deposition rates of carbon on the nickel single-crystalline planes were different.<sup>9</sup> Yang and Chen reported that the most favored face for graphite precipitation of metallic nickel was (111) followed by (110).<sup>10</sup> For our hexagonal-shaped single-crystalline flakes with the bottom/top face of (111) planes and the side faces of (110) planes, the (111) planes were much more abundant than that of (110) planes.<sup>7,11</sup> Therefore, the deposition rates of carbon on nickel flakes were anisotropic, which was possibly the driving force for the growth of coiled graphite layers and further to creviced carbon nanotubes.<sup>12</sup> When the polycrystalline nickel nanoparticles were used as the promoter, the deposition rates of carbon were approximately equal, which led into continuous CNTs. More detailed research on the formation mechanism of the creviced CNTs is in progress.

Figure 3 showed the charge/discharge curves of the EDLSCs fabricated with the above two kinds of CNTs. The creviced CNTs obviously displayed much higher specific capacitance than that of the creviceless CNTs. One charge/discharge cycle time of the creviced CNTs was 600 s, while that of the creviceless CNTs was 334 s. Since that the other conditions were constant, a longer cycle time indicated that a higher amount of electric energy was stored in the EDLC of the creviced CNTs. According to the equation of  $C = i\Delta t/m\Delta V$ , where  $C$  is the ca-

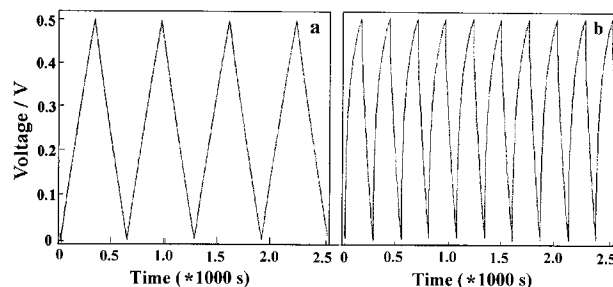


**Figure 3.** The charge–discharge curves (a) multicreviced CNTs, (b) creviceless CNTs promoted by nickel nanoparticles.

pacitance in Farads (F);  $i$  is the discharge current in ampere (A);  $\Delta t$  is the time period (in seconds) for the potential change ( $\Delta V$ , in volts), capacitances of the two samples were calculated as 84 and 44  $F \cdot g^{-1}$ , respectively.<sup>4</sup> Such a value of the creviced CNTs was even much higher than that of the reported “activated” CNTs.<sup>2</sup> The creviced CNTs also showed excellent cyclic stability. From the 1st to the 200th cycle, there was only 0.8% decrease in the capacitance (seen the Supporting Information 2).<sup>14</sup> Due to that the capacitance of CNTs was closely relevant with their specific surface area, the higher capacitance of multi-creviced CNTs could be rationally attributed to the crevices in the tube walls which allowed larger active surface reached by the electrolyte ions.<sup>6</sup> While the good cyclic stability could be attributed to the structural and chemical stability of the CNTs.<sup>13</sup>

In summary, multicreviced CNTs were fabricated by pyrolyzing acetone with anisotropic metallic nickel nanoflakes as catalyst. The anisotropic deposition rates of carbon on the different crystal planes of nickel particles was believed the key factor resulting in the formation of the creviced CNTs. Thus-prepared CNTs exhibited high electrochemical capacitance and good cyclic stability, which was ascribed to their special creviced tube walls accompanying larger surface area accessible by electrolyte ions and higher structural and chemical stability.

## References and Notes

- 1 E. Frackowiak, K. Jurewicz, S. Delpoux, F. Bèguin, *J. Power Sources* **2001**, *97*, 822.
- 2 S. Sarangapani, B. V. Tilak, C. P. Chen, *J. Electrochem. Soc.* **1996**, *143*, 3791.
- 3 Q. Jiang, Y. Zhao, X. Y. Lu, X. T. Zhu, G. Q. Yang, L. J. Song, Y. D. Cai, X. M. Ren, L. Qian, *Chem. Phys. Lett.* **2005**, *410*, 307.
- 4 E. Frakowiak, K. Jurewicz, K. Szotak, S. Delpoux, F. Bèguin, *Fuel Process Technol.* **2002**, *77*, 213.
- 5 Y. Show, K. Imaizumi, *Diamond & Related Mater.* **2006**, *15*, 2086.
- 6 K. Jurewicz, K. Babel, R. Pietrzak, S. Delpoux, H. Wachowska, *Carbon* **2006**, *44*, 2368.
- 7 X. Ni, L. Chen, H. Zheng, D. Zhang, Q. Zhao, J. Song, *Chem. Lett.* **2004**, *33*, 1564.
- 8 M. Endo, Y. A. Kim, T. Hayashi, Y. Fukai, K. Oshida, M. Terrones, T. Yanagisawa, S. Higaki, M. S. Dresselhaus, *Appl. Phys. Lett.* **2002**, *80*, 1267.
- 9 S. Motojima, S. Asakura, T. Kasemura, S. Takeuchi, H. Iwanaga, *Carbon* **1996**, *34*, 289.
- 10 R. T. Yang, J. P. Chen, *J. Catal.* **1989**, *115*, 115.
- 11 X. Ni, Q. Zhao, D. Zhang, X. Zhang, H. Zheng, *J. Phys. Chem. C* **2007**, *111*, 601.
- 12 M. Kawaguchi, K. Nozaki, S. Motojima, H. Iwanaga, *J. Cryst. Growth* **1992**, *118*, 309.
- 13 R. Z. Ma, J. Liang, B. Q. Wei, B. Zhang, C. L. Xu, D. H. Wu, *J. Power Sources* **1999**, *84*, 126.
- 14 Supporting Information is electronically available on the CSJ Journal Web Site, <http://www.csj.jp/journals/chem-lett/>.